ACS OMEGA

Article

http://pubs.acs.org/journal/acsodf

Molecular Insights into Gelation of Di-Fmoc-L-Lysine in Organic Solvent−Water Mixtures

Seyed Meysam Hashemnejad,[†,§] Md Masrul Huda,[†,‡,§] Neeraj Rai,*[,†,‡] and Santanu Kundu*[,†]

[†]Dave C. Swalm School of Chemical Engineering and [‡]Center for Advanced Vehicular Systems, Mississippi State University, Mississippi State, Mississippi 39762, United States

Supporting Information

ABSTRACT: Despite significant interest in molecular gels due to their intriguing structure formation through self-assembly and their stimuli-responsive behavior, our understanding of the gel formation mechanism of a low-molecular-weight gelator (LMWG) is incomplete. Here, we report a combined experimental and computational study on a LMWG, di-Fmoc-L-lysine, that has two aromatic moieties and multiple hydrogen bond donors and acceptors. Gelation in various organic solvent−water mixtures was obtained through the solvent-triggered technique. We show that an approach based on approximate cohesive energy density derived from density functional theory (DFT) calculations can capture the experimental solubility trend of LMWGs in different organic solvents. Furthermore, DFT calculations indicate parallel and helical structures to be the preferred structural motifs for gelator dimers. We believe that these motifs can potentially lead to fiber formation as observed with microscopy. Our work provides a relatively simple yet effective approach to quantify interactions between solvents and complex gelators that can help rationalize solubility and gelation behavior.

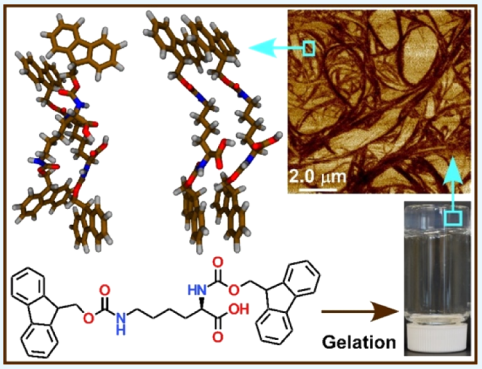

INTRODUCTION

Molecular gels have received significant attention as their stimuli-responsive behavior makes them attractive for numerous applications, including drug delivery, tissue engineering, and nanostructured materials.[1−6] In these systems, low-molecular-weight gelators (LMWGs) are dissolved in a solvent and gelation is triggered by external stimuli such as temperature,[7] ultraviolet light,[8] salt,[9] and pH[10,11] or by changing the solubility of gelators through addition of poor solvents.[12,13] The LMWGs often consist of multiple chemical moieties that manifest different intermolecular interactions between gelator molecules and between gelators and the surrounding media. The interactions ($\sim k_B T$) can be in the form of hydrogen bonding, dispersion, and $\pi-\pi$ interactions.[3,14,15] These relatively weak interactions make the gelation process and gel properties dynamic and complex.[16,17]

The solvent-triggered method is a common method to induce gelation for different aromatic peptide amphiphiles.[13,18−21] In this approach, LWMGs are dissolved in good solvents to obtain a homogeneous solution within a few minutes and then another liquid is added to the solution to trigger gelation. The second liquid is a poor solvent for the gelator but is completely miscible with the first solvent. Using this approach, gelation of Fmoc-peptide gelator molecules in organic solvent−water mixtures has been reported, for example, gelation of Fmoc−leucine−glycine,[18] Fmoc−phenylalanine derivatives,[19] Fmoc−diphenylalanine,[13,20] and Fmoc−asparagine[21] in dimethyl sulfoxide (DMSO)−water. In these systems, parallel and antiparallel stacking of Fmoc moieties result in self-assembled fibrils, ribbons, or other structures.[3,14] The self-assembly process becomes more complex if additional aromatic moieties are present,[10,14,22−25] such as in di-Fmoc-L-lysine in which two Fmoc moieties exist at the two ends of the gelator molecule. This gelator molecule has shown to form gels,[11] but many possible combinations of stacking can be anticipated, and such a self-assembly process cannot be completely elucidated using a phenomenological approach.

In addition to hydrophobic Fmoc moieties, the gelator molecules consist of many functional groups. Interactions between these functional groups and the solution media play an important role in the self-assembly process; however, our understanding on the gel formation mechanism of LWMGs in a particular medium is incomplete.[2,26−28] The most widely used approach, based on the Hansen solubility parameters (HSPs),[26,27,29−33] classifies gelators and solvents depending upon the difference between the respective HSP components, namely, dispersion, polar, and hydrogen bonding. In some instances, HSPs were shown to correlate (or partially correlate) with the gelation behavior of a gelator in a particular solvent.[26,27,29−33] Such correlation mostly involves only one of the HSP components, but the other components do not follow any trend.[27] For instance, 12-hydroxystearic acid (HSA) gelation behavior correlates with the hydrogen bonding component, $\delta_{\text{H-bond}}$, of HSPs.[27] HSA forms gels in solvents

Received: January 30, 2017
Accepted: April 25, 2017
Published: May 5, 2017

DOI: 10.1021/acsomega.7b00108
ACS Omega 2017, 2, 1864−1874

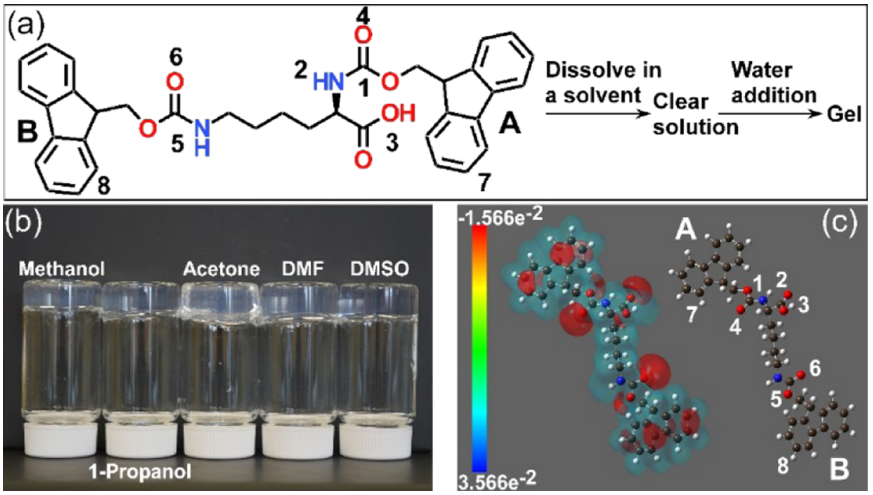

Figure 1. Chemical structure of the gelator with an electrostatic potential map and gel formation. (a) Solvent-triggered gel formation of di-Fmoc-L-lysine, (b) Optical images of inverted 20 mL glass vials containing gels in different solvents. All images were taken 72 h after addition of water. The gelator concentration is 1.7 mM, and the solvent volume fraction, $\phi_{solvent}$, is 0.20, (c) electrostatic potential map (left) and the number system used to identify the location of solvent binding sites (right).

Table 1. Hildebrand Solubility Parameter (SP), Gelator–Solvent Average Binding Energy (U), Pseudo Cohesive Energy Density of the Gelator ($PCED_{g\text{-}s}$) Normalized by the CEDs of the Solvent, Dissolution Temperature of the Gelator in Organic Solvents, and Its Gel Formation upon Addition of Water

solvent	SP ($MPa^{0.5}$)	U (kJ/mol)	$\Lambda = PCED_{g\text{-}s}/CEDs$	$T_{solvation}$ (°C)	gelation
DMF	24.7	50.9	0.167	~22	gel
DMSO	26.4	64.6	0.191	~22	gel
acetone	19.7	39.6	0.211	~22	gel
1-propanol	24.9	42.5	0.141	~50	gel
ethanol	26.2	40.4	0.123	~78	gel
methanol	29.7	39.4	0.094	~50	unstable gel[a]
water	48	36.0	0.035	I[b]	I[b]

[a]Precipitation observed after about 7 days. [b]I: insoluble.

with low $\delta_{H\text{-}bond}$ but remains in solution with high $\delta_{H\text{-}bond}$.[34] However, this approach is not suitable for many cases such as ALS gelators (consisting of aromatic groups other than Fmoc, linkers, and steroidal groups), where gelation does not correlate with any of the HSP components.[27]

Computational approaches such as density functional theory (DFT),[35−37] molecular dynamics,[38−44] and Monte Carlo[40,45] have been used to study the self-assembly of gelators, the preferred geometry of gelators in the gel state, and a priori prediction of gelation.[38,46,47] The ability to predict or to correlate solubility or gelation with the solubility parameter approach rests on the applicability of geometric mixing rules for solvent–gelator interactions.[48,49] Given the difficulty in determining the accurate solubility parameters of complex molecules, especially of gelator molecules that are yet to be synthesized, exploring the utility of DFT calculations to approximate cohesive energy density (CED) is appealing.

The experimental and computation studies in tandem can provide a better understanding of the gel formation mechanism of LMWGs. Toward this goal, we consider the gelation of a LMWG, di-Fmoc-L-lysine or Fmoc-Lys(Fmoc)-OH, in an organic solvent–water mixture. We used the solvent-triggered technique for gelation, in comparison to the earlier report of gelation of this molecule in different pH buffers.[11] The computational approach involves determining the binding energy of organic solvents at selected sites of the gelator molecule. The solubility trend obtained from the computational study correlates with the experimental observation of gelation after addition of water in the gelator solution.

The di-Fmoc-L-lysine molecule has a unique molecular structure (Figure 1), as it has two Fmoc end moieties and multiple functional groups capable of hydrogen bonding. The Fmoc moieties of di-Fmoc-L-lysine can interact with the Fmoc moieties of other gelator molecules through $\pi-\pi$ interactions, and various configurations are possible, for example, parallel and antiparallel stacking,[14] but the most favorable configuration has not been determined. Also, two large aromatic end-groups with dihedral flexibility and the presence of multiple hydrogen bond acceptor and donor groups result in complex interactions that are difficult to predict using the phenomenological approach. DFT calculations presented here provide energetics associated with stacking of two gelator molecules leading to fibrillar and branched structure formation, as observed from microscopy.

RESULTS AND DISCUSSION

Gel Preparation and Characterization. Gels were prepared using the solvent-triggered approach (Figure 1a),[13,18−21] where the gelator was dissolved in an appropriate organic solvent, followed by addition of water. We chose organic solvents with varying polarity and hydrogen bonding capability, such as methanol, ethanol, 1-propanol, DMSO, and dimethylformamide (DMF) (hereby referred as solvents). Water is miscible with the organic solvents but is a poor

DOI: 10.1021/acsomega.7b00108
ACS Omega 2017, 2, 1864−1874

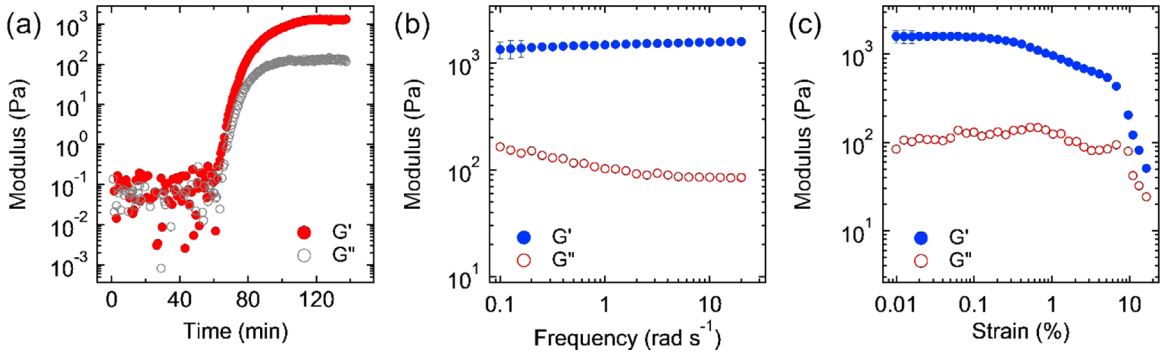

Figure 2. Rheological behavior of a gel in DMF–water with gelator concentration of 3.4 mM and $\phi_{DMF} \approx 0.26$. (a) Evolution of shear moduli as a function of time. Storage and loss moduli as a function of (b) frequency and (c) strain. Measurements were performed immediately after completion of the gelation process.

solvent for the gelator. Dissolving the gelator in the organic solvents resulted in transparent solutions. The solution became opaque with addition of water but turned into a transparent gel after some time. Sequential addition of a solvent and nonsolvent is important for our case, as addition of gelator in a binary mixture of an organic solvent and water did not result into gel formation. Most of the results presented here are for gelator concentrations of 1.7 and 3.4 mM (equivalent to 1 and 2 mg/mL, respectively). The volume fraction of the solvent ($\phi_{solvent}$) in the final solution was maintained as 0.20 or 0.26. The gelator dissolves in DMF, DMSO, and acetone easily, within few minutes and without any external mixing. However, heating and mixing were required to dissolve the gelator in methanol, 1-propanol, and ethanol (see Table 1). Also, the gelation time depends on the solvent; for example, 1-propanol–, DMF–, and acetone–water systems have the fastest gelation time, on the order of 2 h, whereas it took about 2 days in methanol. We also note that gels in methanol–water systems were not very stable, as precipitation of the gelator was observed after about 7 days.

Figure 1b displays the images of the gel samples in different solvents, 72 h after addition of water, as tested by the vial inversion test. We have also attempted to obtain a phase/morphology diagram for these gels.[50−52] The results for three solvents, 1-propanol, acetone, and DMF, are shown in Figure S1. For the 1-propanol and DMF samples, we considered the maximum temperature of 80 °C, whereas for acetone samples, the maximum temperature was 60 °C, near the boiling point of acetone. Phase transition was investigated, through visual observation and the vial inversion test, at every 10 °C interval by heating the samples in an oven. For every temperature, we have waited at least 60 min so that the samples can reach a thermal equilibrium. At low concentration, less than about 0.5 mg/mL, a low-viscosity solution was observed. At room temperature, with increasing gelator concentration, the low-viscosity solution became a viscous solution, similar to that reported by Gao et al.[50] This is followed by gel formation beyond the gelator concentration of about 0.8 mg/mL. With increasing temperature, the gel samples maintained their structural integrity up to a certain temperature, but with a further increase of temperature, the samples started to melt and the samples consisted of two phases, a block of gel in a viscous solution (see Figure S1). With further increase of temperature, the 2-phase samples melted to become fluid. The sol–gel transition temperature in our system does not show a significant concentration dependence.[51] Gelation of small-molecule gelators has been described as a "crystalline assembly" process, a kinetically controlled process.[28,53] Interestingly, the melting behavior of our gel has shown some resemblance to the melting of a semicrystalline polymer with broad melting transition.

Gel formation was further evaluated using shear rheology. Here, the evolution of dynamic moduli, G' (storage modulus) and G'' (loss modulus), was tracked as a function of time.[54] As displayed in Figure 2a, for a gel in DMF–water, G' and G'' increased with time and reached a plateau after about 120 min. At that stage, G' was about an order of magnitude higher than G'', confirming the formation of a gel (soft-solid)-like material. The gel also displays an almost frequency-independent behavior (Figure 2b). Figure 2c displays changes in G' and G'' as a function of strain as obtained from the strain-sweep experiments. Some of these gels display a strain-softening behavior at a relatively low strain amplitude, for example, softening of a gel in DMF–water starts at approximately 0.3% strain amplitude. It is important to note that the gels loss their structural integrity once they are subjected to large strain. The subsequent recovery process, that is, the reformation of a three-dimensional gel structure, is very slow or in some instances (e.g., DMSO) has not been observed even after prolonged wait time over multiple days. A similar slow recovery process has also been observed for the gels melted at elevated temperatures.

Although shear rheology is a common technique to capture the gelation of LMWGs as a function of time, there are several challenges that can affect the results. For example, these gels are quite soft and often dissociate at a small strain (Figure 2c).[25] Therefore, the investigation of the mechanical properties of these gels as a function of strain and frequency needs to be conducted on the samples that are prepared on the rheometer itself (in situ rheology). This process can be time-consuming, and the results can be affected because of drying of solvent during the prolonged gelation time. Alternatively, the cavitation rheology technique can be used.[55] In cavitation rheology experiments, a needle is inserted in a gel sample at an arbitrary location, thus creating a defect within the gel sample at the tip of the needle. The gel at the needle tip is then pressurized using a syringe pump. During pressurization, the system pressure increases with time and at the critical pressure, P_C, the gel sample at the tip of the needle undergoes rapid mechanical deformation, resulting in either elastic instability (cavitation) or fracture of the sample.[56] This process is manifested by a sudden increase in cavity growth (growth of defect) at the tip of the needle. In general, a spherical cavity is observed when the rapid

DOI: 10.1021/acsomega.7b00108
ACS Omega 2017, 2, 1864−1874

deformation is caused by elastic instability, whereas the fracture process causes an irregular growth of cavity. The critical pressure scales with the gel mechanical properties, such as the elastic modulus of the sample (E).[56] Particularly, for elastic instability, considering a neo-Hookean material, $P_C \approx \frac{5E}{6} + \frac{2\gamma}{r_s}$, and for a fracture-like behavior, $P_C \approx \left(\frac{\pi E G_c}{3r_s}\right)^{1/2}$, where γ is the surface energy, r_s is the needle radius or defect size, and G_c is the critical energy release rate, that is, the energy required to create a new surface area during the fracture process.[56] This particular technique does not require any special sample preparation procedure, and the experiments can also provide insights into the fracture behavior of these gels.

Here, the cavitation rheology experiments were conducted on gels for a constant gelator concentration of 1.7 mM and organic solvent volume fraction ($\phi_{solvent}$) of 0.20. Figure 3 displays P_C for different gels and the images of the corresponding defect growth or gel deformation at the needle tip. The P_C values for these gels are similar, indicating no significant difference in low-strain elastic moduli of these gels.

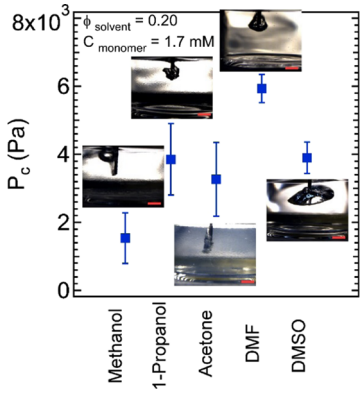

Figure 3. Critical pressure (P_C) for different gels obtained from cavitation rheology experiments. The micrographs illustrate the cavity growth at the tip of the needle. The experiments were conducted at 22 °C and 72 h after addition of water. The inner radius of the needle is ≈156 μm. The scale bar represents 2 mm.

Interestingly, the nature of gel deformation also depends on the solvent used. For all gels, except that in DMSO, the cavity growth was around the needle, extended to the surface. For methanol, the most unstable gel as described above and having the lowest critical pressure, the cavity moved toward the sample surface. In comparison, for the case of DMSO, the cavity remains at the tip of the needle. In all of these cases, the deformation at the tip of the needle can be characterized as fracture. Because fracture is the primary mode of deformation, we can estimate G_c based on the equation provided above. Considering $G' \sim 1$ kPa, G_c is ~0.1 J/m^2, which is significantly smaller than 1−10 J/m^2,[57] typically observed for polymeric gels. Lower values of G_c signify that the gel can fracture relatively easily.

Rationalization of Solubility and Gelation Using the Solubility Parameter Approach. Similar to previous literature reports,[26,30] we attempted to link the solubility parameters of the gelator and solvents to describe the solubility trend and subsequent gel formation. Table 1 presents the Hildebrand solubility parameters for different solvents (HSPs are shown in Table S1 in the Supporting Information).[33] The solubility parameters (square root of the CED) for the gelator are unknown but can be estimated using group contribution theory.[58] We estimated HSPs as $\delta_{dispersion} \approx 27.67$ MPa$^{0.5}$, $\delta_{polar} \approx 10.95$ MPa$^{0.5}$, and $\delta_{H\text{-}bond} \approx 6.93$ MPa$^{0.5}$. Correspondingly, the Hildebrand solubility parameter is estimated as $\sqrt{(\delta_{dispersion}^2 + \delta_{polar}^2 + \delta_{H\text{-}bond}^2)} \approx 30.56$ MPa$^{0.5}$.

For a solid to be soluble in a particular solvent, the solubility parameters of the solid and the solvent need to be similar. On the basis of this rule, we would expect the gelator to have similar solubility in DMSO and ethanol as these solvents have very similar solubility parameters (see Table 1). This is contrary to the experimental observation, where the gelator is readily soluble in DMSO under ambient conditions, whereas we need to heat ethanol to nearly its boiling point to achieve dissolution of the gelator. Although the Hildebrand solubility parameters do not capture the solubility trend of this gelator, several observations can be made from the data presented in Table 1. Dissolution of the gelator in a solvent with high degree of H-bonding is unfavorable. For example, the gelator is insoluble in water, which has the highest $\delta_{H\text{-}bond}$, but it is soluble in 1-propanol, methanol, and ethanol only at an elevated temperature where the H-bond network is not as extensive as that in water. Also, aprotic solvents including DMSO, DMF, and acetone with high $\delta_{dispersion}$ and with no H-bond donating capabilities favor dissolution of gelator. Interestingly, $\delta_{dispersion}$ for the gelator is far away from $\delta_{dispersion}$ for these solvents (see Table S1).

To investigate further, the fate of the gelator after addition of water has been related to the HSPs of the solvents used here (Figures 4 and S2). Following the trend of solubility, aprotic solvents resulted in a stable gel. However, for methanol, which has a high $\delta_{H\text{-}bond}$, the gel is unstable. In comparison, 1-propanol, which has lower $\delta_{H\text{-}bond}$ compared to that of the other alcohols used here, provides a stable gel. The results indicate

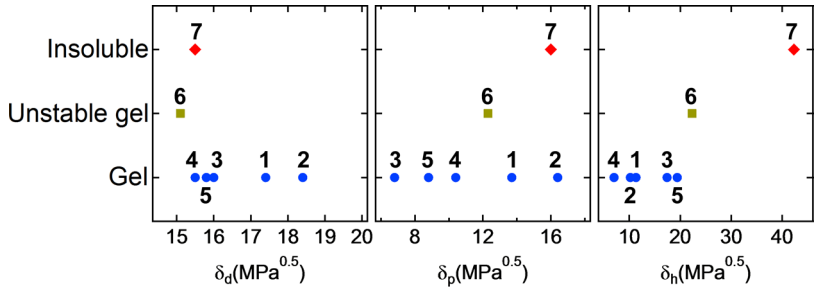

Figure 4. Fate of the gelator in different solvents as a function of HSPs of solvents.

DOI: 10.1021/acsomega.7b00108
ACS Omega 2017, 2, 1864−1874

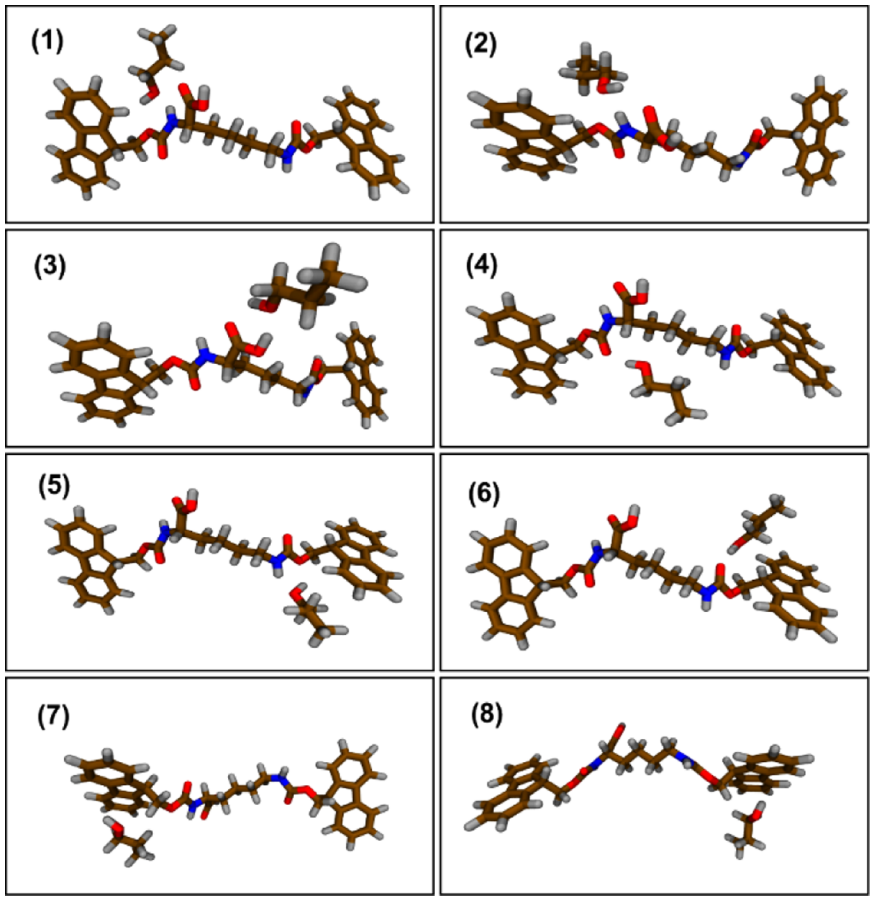

Figure 5. Optimized structure of the 1-propanol molecule (solvent) at different interaction sites around di-Fmoc-L-lysine (gelator).

that the higher degree of H-bonding between solvent molecules interferes with the H-bonding between gelator molecules and therefore playing an important role in gel formation and dictating the stability of the gels. Given the important role of H-bonding and solvent polarity, we also utilized Kamlet–Taft parameters[59−62] and the pyrene-based I_3/I_1 ratio[63] to understand the solubility and gelation trends. These solvatochromic solvent parameters are presented in Tables S4 and S5. The β, π^*, and I_3/I_1 parameters do not show any correlation with the observed solubility trends. For example, acetone and water have virtually identical β parameters (0.43 and 0.47, respectively) but have very different abilities to solubilize the gelator. Similarly, DMSO and water have similar π^* parameters but are at the opposite end of the solubility scale. The I_3/I_1 ratio displays a negative correlation for alcohols considered in the present work. The hydrogen bond donating ability index (α) displays a weak positive correlation. However, the binary nature of this parameter (~0 for molecules without a polar H and ~1 for solvents with a polar H) presents a significant challenge in utilizing this parameter as a useful metric. Furthermore, the α parameter would predict that most nonpolar molecules (with $\alpha \sim 0$) would dissolve the gelator, which is contrary to the observation that di-Fmoc-L-lysine is not soluble in hexane.

The use of solubility parameter for capturing the solubility/gelation rests on the assumption that the binary interaction between the gelator and solvent can be approximated with the geometric mixing rule.[48,49] It has been shown that the geometric mixing rule appears inadequate when molecules differ significantly in their size as is the case in the present work.[64,65] To overcome this limitation, we calculated the binary interaction between the gelator and solvent using DFT. Ideally, one would carry out a detailed molecular simulation to calculate the solute–solvent interaction, but this will be an extremely time-consuming process.[66] Furthermore, classical simulations rely on empirical force fields and their accuracy can sometimes be suspect unless there is significant experimental data to validate the accuracy of the force field. For this reason, we took an approach that does not rely on empirical force fields and that does not require extensive computational resources.

We employed hybrid DFT to calculate the binary interaction between the gelator and solvent at different binding sites. We selected different binding sites (total of eight) based on the electrostatic potential map of the gelator (see Figures 1c and 5, which show optimized geometries of the propanol-gelator at different sites). As can be seen from Figure 1c, the negative electronic charge density or more polarizable regions of the space depicted in red color are near the oxygen atoms in the functional groups as well as at the aromatic groups.

In addition to elucidating the different energetic contributions to the gelator–solvent interaction, this computational approach allows us to calculate a reasonable estimate of the gelator–solvent binding energy at different binding sites (Table S2). From Table S2, it is evident that the site for the strongest binding is different for protic and aprotic solvents. Protic solvents (water and alcohols) interact strongly with the acidic functional group at site 3, whereas aprotic solvents interact strongly with the amide group at site 6 (see Figures 5 and S3). This is because aprotic solvents at site 6 can maximize the interaction by orienting such that they can form a weak H-bond with the acid group at site 3, whereas this is not possible for a

DOI: 10.1021/acsomega.7b00108
ACS Omega 2017, 2, 1864−1874

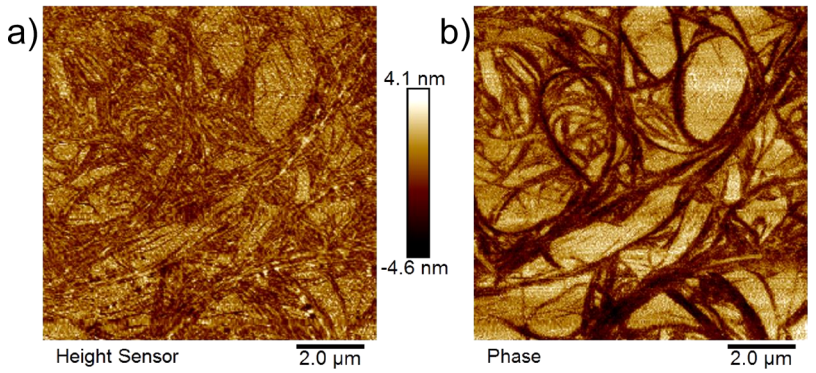

Figure 6. AFM image of a wet gel in the DMF−water system using the tapping mode. Height data is shown in (a), whereas the phase image is shown in (b). The gelator concentration is 3.4 mM and $\phi_{DMF} \approx 0.26$.

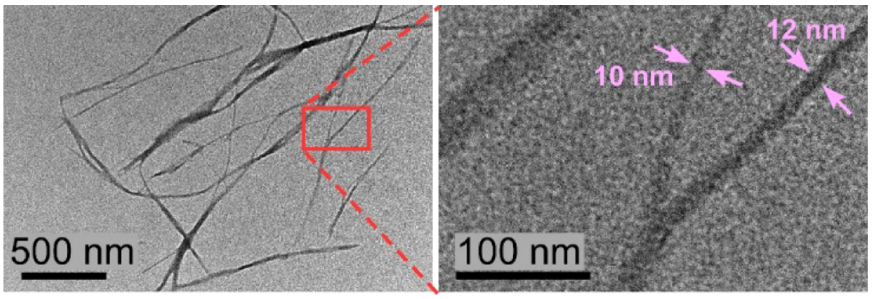

Figure 7. TEM images of gel in 1-propanol−water at two different locations. The gelator concentration is 1.7 mM and $\phi_{1\text{-propanol}} \approx 0.26$.

protic solvent. An arithmetic average of the binding energy at 8 binding sites provides us the average binding energy, U (kJ/mol). The molecular volume (cm^3/mol) of the gelator−solvent system at different binding sites (see Figure 5 in the case of the *n*-propanol molecule and Figure S3 for the DMSO molecule) is also calculated (ϑ_M) and was used to obtain pseudo cohesive energy density of the gelator−solvent binary mixture as $PCED_{g-s} = \sqrt{U/\vartheta_M}$. This is a measure of the binding energy per unit volume and has the same unit as that of CED. The cohesive energy of a solvent quantifies the energy gained when individual molecules associate to form one mole of condensed phase.[48,49] It is necessary to normalize this quantity with the molar volume as larger molecules will generally have larger cohesive energy on a molar basis. This leads to CED, which is used to calculate the solubility parameter. Although one can determine these quantities for organic solvents through enthalpy of vaporization, it is difficult to estimate CED for polymers or for molecules such as LMWGs that generally have low vapor pressure.[67] Here, we are avoiding this by directly calculating the solvent/gelator CED. Because we are not considering the complete solvation sphere, we term this quantity PCED.

The binding energy of the solvent and the molecular volume with the solvent at different binding sites are provided in Tables S2 and S3, whereas in Table 1, we provide the average binding energy (U) and Λ, which is PCED of the gelator−solvent ($PCED_{g-s}$) normalized by the CED of the solvent, that is, $\Lambda = PCED_{g-s}/CED_s$. Λ is a measure of the strength of the gelator−solvent interaction compared to that of solvent−solvent interactions. As displayed in Table 1, the average binding energy of the solvent (U) has a weak correlation with the solubility and gelation characteristics. Experimentally, acetone, DMSO, and DMF are found to be good solvents for di-Fmoc-L-lysine, whereas water is a poor solvent. Although the maximum binding energy (see Table S2) also correlates with the solubility and gelation, but distinction between the solvents is not as pronounced. This suggests that selecting a single interaction site is not a good choice especially for large gelator molecules. The best correlation with the solubility is obtained with respect to Λ. When using Λ, we have very clear distinction between not only gelating and nongelating solvents but also a nongelating solvent and a solvent that results in an unstable gel. As displayed in Table 1, the distinction between methanol that forms an unstable gel and water that forms precipitate is very clear (0.094 vs 0.035).

Microstructure of Molecular Gels. Addition of water triggers nucleation of the gelator followed by growth in the single and/or multiple dimensions via noncovalent interactions between gelator molecules. To elucidate the gel structure, atomic force microscopy (AFM) characterization was conducted on the gel samples in the wet state, which has rarely been reported in the literature. The main advantage of this approach is that sample preparation techniques including drying, freezing, and staining that can potentially introduce some artifacts were not applied. Figure 6a displays the tapping-mode AFM height image and Figure 6b displays the phase image of a gel in DMF−water after 2 h of water addition. The phase image can distinguish various phases present in the system on the basis of their chemical and physical properties captured through the phase shifts of the response signal with respect to the applied signal. A fibrous structure has been observed in the height image; however, the structure is clearly visible in the phase image because of a higher contrast. AFM results indicate that the self-assembled fibers form bundles.

In addition, transmission electron microscopy (TEM) investigations were conducted on the gel samples and the results for the gels in 1-proponal and in DMSO are presented

DOI: 10.1021/acsomega.7b00108
ACS Omega 2017, 2, 1864−1874

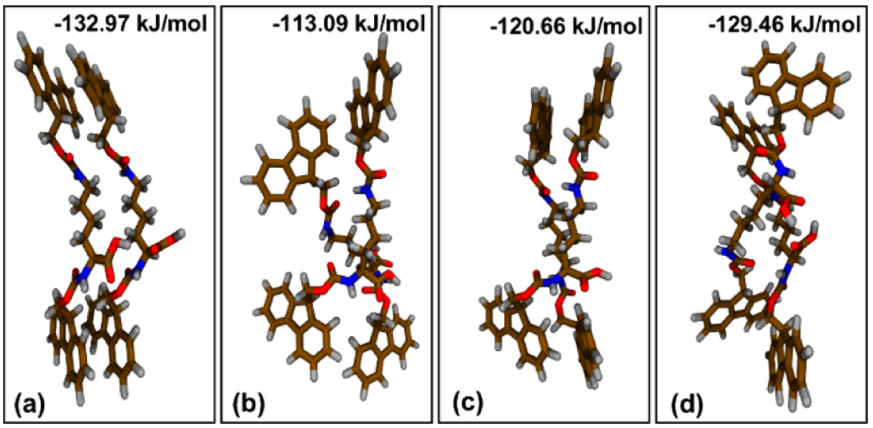

Figure 8. Optimized dimer configurations and their corresponding binding energies. (a) AA−BB parallel stacking, (b) AA−BB Y-shaped stacking, (c) AB−BA mixed stacking, and (d) AB−BA Y-shaped stacking.

in Figures 7 and Figures S4 and S5, respectively. Here, the individual fibers have been imaged. For both these gels, we have found the fiber diameter of ∼10 nm, similar to that reported in the literature for other Fmoc-containing gelators.[12] As estimated from the optimized structure of the gelator molecule, the end-to-end distance is ≈2.3 nm and the width is ≈0.85 nm. This indicates about 10 molecules stack laterally to form these fibers. TEM images also provide evidence of branched fiber growth similar to that observed for some peptide molecules.[68,69]

To understand early aggregation, we performed structural optimization of the gelator dimer using DFT. A dimer can provide important insights into early stage aggregation without requiring extensive computation resources. Aromatic moieties can orient in parallel/parallel-displaced or T/Y-shaped configuration (perpendicular or vertically tilted).[70−72] In the case of benzene, both parallel-displaced and T/Y configurations are nearly isoenergetic.[73] However, it is expected that large rings will favor a parallel or near-parallel configuration so that rings can maximize $\pi-\pi$ interactions. In the case of di-Fmoc-L-lysine, there is also potential for hydrogen bonding along the aliphatic segment that contains acid and amide functional groups. The overall structure of the initial aggregate will be governed by interplay of primarily H-bond and $\pi-\pi$ interactions. Thus, four different initial conformations were chosen, AA−BB and AB−BA both arrangements can stack in parallel and in Y-shaped configuration (A and B are the aromatic rings of the Fmoc moiety, as shown in Figure 1c).

Figure 8 presents the final optimized geometries of the dimers. The most stable dimer structure (binding energy = 132.97 kJ/mol) is obtained when the two aromatic moieties maximize their $\pi-\pi$ interactions through parallel stacking and the carboxylic group of one of the molecules interacts with the carboxylic and amine group of the other molecule via hydrogen bonding (Figure 8a).

The second most stable structure is the case (Figure 8d) where the dimers stacked helically. This structure is structurally very different compared to the most stable structure, but energetically it differs by only about 3 kJ/mol. In this case, the aromatic moieties are perpendicular to one another (Y-shape), while only the carboxylic groups of both molecules participated in the hydrogen bond formation (Figure 8d). In the Supporting Information, we have presented movie files that provide a three-dimensional view of the optimized geometries. On the basis of the dimer energetics, we speculate that two lowest energy structures possibly lead to fiber formation and branching in the gel.

We have not conducted any experimental investigations to study the initial stage of structure formation. However, several observations can be made on the basis of the results provided here. The strain-softening behavior at low strain and the slow recovery process after application of large strain supports the "crystalline assembly" process of gelation, a kinetically controlled process.[28,53] It has been hypothesized that initially the gelator molecules form protofibrils, which then self-assemble to form fibers.[28,74] However, recent results on the NapFFKYp gelator in water display a distinctly different behavior, in which the fibers are formed even with the low gelator concentration and in the solution phase. In future, we intend to investigate early-stage fiber growth through large-scale modeling studies and experiments using small-angle scattering techniques.

CONCLUSIONS

Here, gelation of di-Fmoc-L-lysine in various aprotic and polar solvents and water mixtures using the solvent-triggered method has been achieved. Gels in different solvent systems display similar mechanical responses, as characterized using cavitation rheology. The computational approach adopted here successfully captures the dissolution of the gelator in various organic solvents. A descriptor, Λ, which is defined as the PCED of the gelator−solvent normalized to the CED of the solvent, appears to successfully correlate with the solubility and gelation characteristics of the gelator molecule. Furthermore, a fibrous structure was captured using AFM in the native gel state. DFT calculations indicate that the parallel and helical stackings of aromatic gelator molecules are more stable orientations and these stackings might enable fiber growth that results in a three-dimensional fibrillar network observed with AFM. The experimental and computational approach applied here can be useful not only in the field of molecular gelation but also in any organic self-assembled system and in predicting the solubility of solids in liquids.

Understanding the solubility and gelation characteristics of gelators with multifunctional moieties with hydrogen bonds, polarity, and $\pi-\pi$ interaction presents a significant challenge when utilizing common empirical parameters such as solubility and/or solvatochromatic parameters. We believe that our approach that utilizes DFT to quantify the interaction strength of the solvent and gelator can be a useful tool in rationalizing

DOI: 10.1021/acsomega.7b00108
ACS Omega 2017, 2, 1864−1874

the solubility and self-assembly behaviors of complex gelator molecules.

METHODS

Materials. Di-Fmoc-L-lysine, methanol, ethanol, and 1-propanol were obtained from Sigma-Aldrich and were used as received. DMSO, DMF, and acetone were obtained from Fisher-Scientific. All solvents are of high purity (~99.9%). Deionized water with resistivity of 18.2 mΩ was used for gel preparation.

Gel Formation Protocol. Hydrogels were prepared in a two-step process. The gelator was first dissolved in the solvent of interest (such as DMF, DMSO, acetone, methanol, ethanol, and 1-propanol) and then water was added. The final volume fraction of the solvent ($\phi_{solvent}$ = organic solvent volume/total volume) was fixed either at $\phi_{solvent}$ ≈0.20 or ≈0.26. The gelator concentration was also fixed at 1.7 and 3.4 mM for rheological and microstructural studies. To obtain the phase diagrams, additional samples with varying gelator concentration from 0.1 to 5 mg/mL were prepared. To obtain a gel with 1.7 mM gelator concentration, 5 mg of gelator was dissolved in 1 mL of solvent ($\phi_{solvent}$ ≈ 0.20) followed by addition of 4 mL of water. The gelator dissolved easily in DMF, DMSO, and acetone within 10 min. For methanol and 1-propanol, the samples were heated to 50 °C, whereas for ethanol, the sample was heated near to its boiling temperature of 78 °C. Once the sample reached the desired temperature, the sample was removed from the hot plate and a vortex mixer was used for mixing. Heating and mixing were conducted multiple times until an optically clear solution was obtained. The mixing process was completed in about 30 min. After mixing of gelator, the solution was allowed to cool to room temperature (~22 °C) and water was added at that temperature. Addition of water turned the clear solution to an opaque solution in all cases. Then, all of the samples were either molded or transferred into a rheometer.

TEM. TEM images were obtained using a JEOL LaB6 transmission electron microscope operating at 200 keV. Carbon-coated copper grids (mesh size of 200) were placed on the freshly prepared surfaces for a minute. The grids were then removed and were dried under vacuum after carefully removing excess gel using a filter paper.

AFM. AFM images were obtained at room temperature using a Bruker AFM in TappingMode with the Sharp Nitride Lever (SNL-10) probe, purchased from Bruker. The samples were casted in an aluminum mold and were directly imaged with no specific sample preparation steps. AFM scans were conducted at 512 × 512 pixel resolution and a scanning rate of 1 Hz, and height data were also first-order flattened.

Shear Rheology. Dynamic rheological experiments were performed using a Discovery Hybrid Rheometer (HR2), TA instruments. The samples were transferred to the rheometer after addition of water. A parallel-plate fixture (20 mm) with a solvent trap was utilized for rheological investigations. The evolution of gel formation as a function of time was captured using small-amplitude oscillatory shear experiments at a strain amplitude of 0.1% and a frequency of 5 rad s^{-1}. The gap size was fixed at ~1500 μm. The experiments were performed at least three times and representative results were displayed.

Cavitation Rheology. A custom-built cavitation rheology setup was used to determine the mechanical properties of the gels and to capture the defect growth inside the sample.[55] All experiments were performed after 72 h of water addition and at room temperature. A flat tip needle with inner radius of ≈156 μm (gauge number 24, Hamilton) was used. Measurements were conducted with air as a cavitation media and with a compression rate of 2 mL/min. Cavitation experiments were conducted minimum three times, and the error bars represent one standard deviation.

Computational Details. All calculations were carried out using the Gaussian09 quantum chemistry software package.[75] Because of torsional flexibility, the gelator molecule can take different optimized geometries depending upon initial conformations. Eight optimized geometries were generated; only the energetically most favorable conformation was picked to perform binding energy calculations. The M06-2X[76] density functional and the (6-311+g**)[77,78] basis set were used to optimize the geometries for solvent−monomer systems and to calculate binding energy. An ultrafine grid was used for numerical integration. During the gelator dimer geometry optimization, first, a smaller basis set and then gradually larger basis sets were employed in the following order: (6-31g*),[79,80] (6-311g*),[77,78] and (6-311g**)[77,78] to avoid SCF convergence failure. The frequency calculation was carried out for each geometry optimization to ensure that the final structure is a minima (lack of imaginary frequency).

ASSOCIATED CONTENT

Supporting Information

The Supporting Information is available free of charge on the ACS Publications website at DOI: 10.1021/acsomega.7b00108.

Phase diagram; fate of gelator in different solvents as a function of HSPs; optimized geometries of the DMSO molecule at different interaction sites; TEM images of the gel in the 1-propanol−water mixture and in DMSO−water; HSPs for different organic media used in a binary mixture; binding energies (kJ/mol) of different solvents with the monomer at different interaction sites; molecular volume (cm^3/mol) of different solvents with the monomer at different interaction sites; Kamlet−Taft solvatochromic parameters for solvents; I_3/I_1 ratio of pyrene in neat solvents (PDF)

Movie files that provide a three-dimensional view of the dimer structure (AVI) (AVI) (AVI) (AVI)

AUTHOR INFORMATION

Corresponding Authors

*E-mail: neerajrai@che.msstate.edu (N.R.).

*E-mail: santanukundu@che.msstate.edu (S.K.).

ORCID

Neeraj Rai: 0000-0002-0058-9623

Santanu Kundu: 0000-0002-0767-0512

Author Contributions

§S.M.H. and M.M.H. contributed equally.

Author Contributions

The manuscript was written through contributions of all authors. All authors have given approval to the final version of the manuscript. S.M.H. and S.K. designed the experiments and analyzed the experimental data. S.M.H. performed the experiments. M.M.H. and N.R. designed the computational research and analyzed the data. M.M.H. performed the electronic structure calculations. All authors contributed to discussions and to writing the manuscript.

Notes

The authors declare no competing financial interest.

DOI: 10.1021/acsomega.7b00108
ACS Omega 2017, 2, 1864−1874

■ ACKNOWLEDGMENTS

S.M.H. and S.K. acknowledge financial support from the National Science Foundation [IIA-1430364] and [DMR-1352572] and for the experimental aspects of the manuscript. N.R. acknowledges partial financial support from the National Science Foundation [IIA-1430364] for the computational aspects of the manuscript. All computational work utilized computational resources of High Performance Computing Collaboratory at Mississippi State University.

■ REFERENCES

(1) Mart, R. J.; Osborne, R. D.; Stevens, M. M.; Ulijn, R. V. Peptide-Based Stimuli-Responsive Biomaterials. *Soft Matter* **2006**, *2*, 822−835.
(2) Raghavan, S. R.; Douglas, J. F. The Conundrum of Gel Formation by Molecular Nanofibers, Wormlike Micelles, and Filamentous Proteins: Gelation without Cross-Links? *Soft Matter* **2012**, *8*, 8539−8546.
(3) Raeburn, J.; Cardoso, A. Z.; Adams, D. J. The Importance of the Self-Assembly Process to Control Mechanical Properties of Low Molecular Weight Hydrogels. *Chem. Soc. Rev.* **2013**, *42*, 5143−5156.
(4) Yang, Z.; Xu, K.; Wang, L.; Gu, H.; Wei, H.; Zhang, M.; Xu, B. Self-Assembly of Small Molecules Affords Multifunctional Supramolecular Hydrogels for Topically Treating Simulated Uranium Wounds. *Chem. Commun.* **2005**, *35*, 4414−4416.
(5) Guan, X.; Fan, K.; Gao, T.; Ma, A.; Zhang, B.; Song, J. A Novel Multi-Stimuli Responsive Gelator Based on D-Gluconic Acetal and Its Potential Applications. *Chem. Commun.* **2016**, *52*, 962−965.
(6) Liu, Z.-X.; Feng, Y.; Yan, Z.-C.; He, Y.-M.; Liu, C.-Y.; Fan, Q.-H. Multistimuli Responsive Dendritic Organogels Based on Azobenzene-Containing Poly(aryl Ether) Dendron. *Chem. Mater.* **2012**, *24*, 3751−3757.
(7) Yan, X.; Cui, Y.; He, Q.; Wang, K.; Li, J. Organogels Based on Self-Assembly of Diphenylalanine Peptide and Their Application To Immobilize Quantum Dots. *Chem. Mater.* **2008**, *20*, 1522−1526.
(8) Raeburn, J.; McDonald, T. O.; Adams, D. J. Dipeptide Hydrogelation Triggered via Ultraviolet Light. *Chem. Commun.* **2012**, *48*, 9355−9357.
(9) Chen, L.; Pont, G.; Morris, K.; Lotze, G.; Squires, A.; Serpell, L. C.; Adams, D. J. Salt-Induced Hydrogelation of Functionalised-Dipeptides at High pH. *Chem. Commun.* **2011**, *47*, 12071−12073.
(10) Tang, C.; Smith, A. M.; Collins, R. F.; Ulijn, R. V.; Saiani, A. Fmoc-Diphenylalanine Self-Assembly Mechanism Induces Apparent pKa Shifts. *Langmuir* **2009**, *25*, 9447−9453.
(11) Reddy, S. M. M.; Shanmugam, G.; Duraipandy, N.; Kiran, M. S.; Mandal, A. B. An Additional Fluorenylmethoxycarbonyl (Fmoc) Moiety in Di-Fmoc-Functionalized L-Lysine Induces pH-Controlled Ambidextrous Gelation with Significant Advantages. *Soft Matter* **2015**, *11*, 8126−8140.
(12) Dudukovic, N. A.; Zukoski, C. F. Evidence for Equilibrium Gels of Valence-Limited Particles. *Soft Matter* **2014**, *10*, 7849−7856.
(13) Raeburn, J.; Mendoza-Cuenca, C.; Cattoz, B. N.; Little, M. A.; Terry, A. E.; Cardoso, A. Z.; Griffiths, P. C.; Adams, D. J. The Effect of Solvent Choice on the Gelation and Final Hydrogel Properties of Fmoc−diphenylalanine. *Soft Matter* **2015**, *11*, 927−935.
(14) Fleming, S.; Ulijn, R. V. Design of Nanostructures Based on Aromatic Peptide Amphiphiles. *Chem. Soc. Rev.* **2014**, *43*, 8150−8177.
(15) Ma, M.; Kuang, Y.; Gao, Y.; Zhang, Y.; Gao, P.; Xu, B. Aromatic−Aromatic Interactions Induce the Self-Assembly of Pentapeptidic Derivatives in Water To Form Nanofibers and Supramolecular Hydrogels. *J. Am. Chem. Soc.* **2010**, *132*, 2719−2728.
(16) Wang, J.; Liu, K.; Yan, L.; Wang, A.; Bai, S.; Yan, X. Trace Solvent as a Predominant Factor To Tune Dipeptide Self-Assembly. *ACS Nano* **2016**, *10*, 2138−2143.
(17) Wu, Y.; Wu, S.; Zou, G.; Zhang, Q. Solvent Effects on Structure, Photoresponse and Speed of Gelation of a Dicholesterol-Linked Azobenzene Organogel. *Soft Matter* **2011**, *7*, 9177−9183.
(18) Chen, L.; Raeburn, J.; Sutton, S.; Spiller, D. G.; Williams, J.; Sharp, J. S.; Griffiths, P. C.; Heenan, R. K.; King, S. M.; Paul, A.; et al. Tuneable Mechanical Properties in Low Molecular Weight Gels. *Soft Matter* **2011**, *7*, 9721−9727.
(19) Ryan, D. M.; Anderson, S. B.; Nilsson, B. L. The Influence of Side-Chain Halogenation on the Self-Assembly and Hydrogelation of Fmoc-Phenylalanine Derivatives. *Soft Matter* **2010**, *6*, 3220−3231.
(20) Zhu, P.; Yan, X.; Su, Y.; Yang, Y.; Li, J. Solvent-Induced Structural Transition of Self-Assembled Dipeptide: From Organogels to Microcrystals. *Chem. − Eur. J.* **2010**, *16*, 3176−3183.
(21) Zhang, Y.; Li, S.; Ma, M.; Yang, M.; Wang, Y.; Hao, A.; Xing, P. Tuning of Gel Morphology with Supramolecular Chirality Amplification Using a Solvent Strategy Based on an Fmoc-Amino Acid Building Block. *New J. Chem.* **2016**, *40*, 5568−5576.
(22) Tao, K.; Levin, A.; Adler-Abramovich, L.; Gazit, E. Fmoc-Modified Amino Acids and Short Peptides: Simple Bio-Inspired Building Blocks for the Fabrication of Functional Materials. *Chem. Soc. Rev.* **2016**, *45*, 3935−3953.
(23) Hirst, A. R.; Roy, S.; Arora, M.; Das, A. K.; Hodson, N.; Murray, P.; Marshall, S.; Javid, N.; Sefcik, J.; Boekhoven, J.; et al. Biocatalytic Induction of Supramolecular Order. *Nat. Chem.* **2010**, *2*, 1089−1094.
(24) Jayawarna, V.; Ali, M.; Jowitt, T. A.; Miller, A. F.; Saiani, A.; Gough, J. E.; Ulijn, R. V. Nanostructured Hydrogels for Three-Dimensional Cell Culture Through Self-Assembly of Fluorenylmethoxycarbonyl−Dipeptides. *Adv. Mater.* **2006**, *18*, 611−614.
(25) Sutton, S.; Campbell, N. L.; Cooper, A. I.; Kirkland, M.; Frith, W. J.; Adams, D. J. Controlled Release from Modified Amino Acid Hydrogels Governed by Molecular Size or Network Dynamics. *Langmuir* **2009**, *25*, 10285−10291.
(26) Bonnet, J.; Suissa, G.; Raynal, M.; Bouteiller, L. Organogel Formation Rationalized by Hansen Solubility Parameters: Dos and Don'ts. *Soft Matter* **2014**, *10*, 3154−3160.
(27) Lan, Y.; Corradini, M. G.; Weiss, R. G.; Raghavan, S. R.; Rogers, M. A. To Gel or Not to Gel: Correlating Molecular Gelation with Solvent Parameters. *Chem. Soc. Rev.* **2015**, *44*, 6035−6058.
(28) Douglas, J. F. Theoretical Issues Relating to Thermally Reversible Gelation by Supermolecular Fiber Formation. *Langmuir* **2009**, *25*, 8386−8391.
(29) Raynal, M.; Bouteiller, L. Organogel Formation Rationalized by Hansen Solubility Parameters. *Chem. Commun.* **2011**, *47*, 8271−8273.
(30) Diehn, K. K.; Oh, H.; Hashemipour, R.; Weiss, R. G.; Raghavan, S. R. Insights into Organogelation and Its Kinetics from Hansen Solubility Parameters. Toward a Priori Predictions of Molecular Gelation. *Soft Matter* **2014**, *10*, 2632−2640.
(31) Lan, Y.; Corradini, M. G.; Rogers, M. A. Do Molecular Gelators Cluster in Hansen Space? *Cryst. Growth Des.* **2014**, *14*, 4811−4818.
(32) Yan, N.; Xu, Z.; Diehn, K. K.; Raghavan, S. R.; Fang, Y.; Weiss, R. G. How Do Liquid Mixtures Solubilize Insoluble Gelators? Self-Assembly Properties of Pyrenyl-Linker-Glucono Gelators in Tetrahydrofuran−Water Mixtures. *J. Am. Chem. Soc.* **2013**, *135*, 8989−8999.
(33) Hansen, C. M. *Hansen Solubility Parameters: A User's Handbook*, 2nd ed.; CRC Press: Boca Raton, 2007; pp 27−44.
(34) Gao, J.; Wu, S.; Rogers, M. A. Harnessing Hansen Solubility Parameters to Predict Organogel Formation. *J. Mater. Chem.* **2012**, *22*, 12651−12658.
(35) Bernet, A.; Albuquerque, R. Q.; Behr, M.; Hoffmann, S. T.; Schmidt, H.-W. Formation of a Supramolecular Chromophore: A Spectroscopic and Theoretical Study. *Soft Matter* **2012**, *8*, 66−69.
(36) Li, J.; Fan, K.; Niu, L.; Li, Y.; Song, J. Effects of Salt on the Gelation Mechanism of a D-Sorbitol-Based Hydrogelator. *J. Phys. Chem. B* **2013**, *117*, 5989−5995.
(37) Setnička, V.; Nový, J.; Böhm, S.; Sreenivasachary, N.; Urbanová, M.; Volka, K. Molecular Structure of Guanine-Quartet Supramolecular Assemblies in a Gel-State Based on a DFT Calculation of Infrared and Vibrational Circular Dichroism Spectra. *Langmuir* **2008**, *24*, 7520−7527.
(38) Frederix, P. W. J. M.; Scott, G. G.; Abul-Haija, Y. M.; Kalafatovic, D.; Pappas, C. G.; Javid, N.; Hunt, N. T.; Ulijn, R. V.; Tuttle, T. Exploring the Sequence Space for (Tri-)Peptide Self-

DOI: 10.1021/acsomega.7b00108
ACS Omega 2017, 2, 1864−1874

Assembly to Design and Discover New Hydrogels. *Nat. Chem.* **2015**, *7*, 30−37.
(39) Sasselli, I. R.; Ulijn, R. V.; Tuttle, T. CHARMM Force Field Parameterization Protocol for Self-Assembling Peptide Amphiphiles: The Fmoc Moiety. *Phys. Chem. Chem. Phys.* **2016**, *18*, 4659−4667.
(40) Lu, P. J.; Zaccarelli, E.; Ciulla, F.; Schofield, A. B.; Sciortino, F.; Weitz, D. A. Gelation of Particles with Short-Range Attraction. *Nature* **2008**, *453*, 499−503.
(41) Corezzi, S.; Michele, C. D.; Zaccarelli, E.; Fioretto, D.; Sciortino, F. A Molecular Dynamics Study of Chemical Gelation in a Patchy Particle Model. *Soft Matter* **2008**, *4*, 1173−1177.
(42) Guo, C.; Arnon, Z. A.; Qi, R.; Zhang, Q.; Adler-Abramovich, L.; Gazit, E.; Wei, G. Expanding the Nanoarchitectural Diversity Through Aromatic Di- and Tri-Peptide Coassembly: Nanostructures and Molecular Mechanisms. *ACS Nano* **2016**, *10*, 8316−8324.
(43) Jang, S.; Yuan, J.-M.; Shin, J.; Measey, T. J.; Schweitzer-Stenner, R.; Li, F.-Y. Energy Landscapes Associated with the Self-Aggregation of an Alanine-Based Oligopeptide (AAKA)4. *J. Phys. Chem. B* **2009**, *113*, 6054−6061.
(44) Sasselli, I. R.; Pappas, C. G.; Matthews, E.; Wang, T.; Hunt, N. T.; Ulijn, R. V.; Tuttle, T. Using Experimental and Computational Energy Equilibration to Understand Hierarchical Self-Assembly of Fmoc-Dipeptide Amphiphiles. *Soft Matter* **2016**, *12*, 8307−8315.
(45) Li, M. S.; Klimov, D. K.; Straub, J. E.; Thirumalai, D. Probing the Mechanisms of Fibril Formation Using Lattice Models. *J. Chem. Phys.* **2008**, *129*, No. 175101.
(46) Gupta, J. K.; Adams, D. J.; Berry, N. G. Will It Gel? Successful Computational Prediction of Peptide Gelators Using Physicochemical Properties and Molecular Fingerprints. *Chem. Sci.* **2016**, *7*, 4713.
(47) Veits, G. K.; Carter, K. K.; Cox, S. J.; McNeil, A. J. Developing a Gel-Based Sensor Using Crystal Morphology Prediction. *J. Am. Chem. Soc.* **2016**, *138*, 12228−12233.
(48) Hildebrand, J. H. The Entropy of Solution of Molecules of Different Size. *J. Chem. Phys.* **1947**, *15*, 225−228.
(49) Scatchard, G. Equilibrium in Non-Electrolyte Mixtures. *Chem. Rev.* **1949**, *44*, 7−35.
(50) Gao, Y.; Nieuwendaal, R.; Dimitriadis, E. K.; Hammouda, B.; Douglas, J. F.; Xu, B.; Horkay, F. Supramolecular Self-Assembly of a Model Hydrogelator: Characterization of Fiber Formation and Morphology. *Gels* **2016**, *2*, No. 27.
(51) Mitra, R. N.; Das, D.; Roy, S.; Das, P. K. Structure and Properties of Low Molecular Weight Amphiphilic Peptide Hydrogelators. *J. Phys. Chem. B* **2007**, *111*, 14107−14113.
(52) Terech, P.; Weiss, R. G. Low Molecular Mass Gelators of Organic Liquids and the Properties of Their Gels. *Chem. Rev.* **1997**, *97*, 3133−3160.
(53) Raghavan, S. R. Distinct Character of Surfactant Gels: A Smooth Progression from Micelles to Fibrillar Networks. *Langmuir* **2009**, *25*, 8382−8385.
(54) Hashemnejad, S. M.; Kundu, S. Strain Stiffening and Negative Normal Stress in Alginate Hydrogels. *J. Polym. Sci., Part B: Polym. Phys.* **2016**, *54*, 1767−1775.
(55) Hashemnejad, S. M.; Kundu, S. Nonlinear Elasticity and Cavitation of a Triblock Copolymer Gel. *Soft Matter* **2015**, *11*, 4315−4325.
(56) Kundu, S.; Crosby, A. J. Cavitation and Fracture Behavior of Polyacrylamide Hydrogels. *Soft Matter* **2009**, *5*, 3963−3968.
(57) Gong, J. P. Why Are Double Network Hydrogels so Tough? *Soft Matter* **2010**, *6*, 2583−2590.
(58) Stefanis, E.; Panayiotou, C. Prediction of Hansen Solubility Parameters with a New Group-Contribution Method. *Int. J. Thermophys.* **2008**, *29*, 568−585.
(59) Yokoyama, T.; Taft, R. W.; Kamlet, M. J. The Solvatochromic Comparison Method. 3. Hydrogen Bonding by Some 2-Nitroaniline Derivatives. *J. Am. Chem. Soc.* **1976**, *98*, 3233−3237.
(60) Lan, Y.; Corradini, M. G.; Liu, X.; May, T. E.; Borondics, F.; Weiss, R. G.; Rogers, M. A. Comparing and Correlating Solubility Parameters Governing the Self-Assembly of Molecular Gels Using 1,3:2,4-Dibenzylidene Sorbitol as the Gelator. *Langmuir* **2014**, *30*, 14128−14142.
(61) Brune, B. J.; Payne, G. F.; Chaubal, M. V. Linear Solvation Energy Relationships To Explain Interactions Responsible for Solute Adsorption onto a Polar Polymeric Sorbent. *Langmuir* **1997**, *13*, 5766−5769.
(62) Edwards, W.; Lagadec, C. A.; Smith, D. K. Solvent−gelator Interactions—using Empirical Solvent Parameters to Better Understand the Self-Assembly of Gel-Phase Materials. *Soft Matter* **2011**, *7*, 110−117.
(63) Amiji, M. M. Pyrene Fluorescence Study of Chitosan Self-Association in Aqueous Solution. *Carbohydr. Polym.* **1995**, *26*, 211−213.
(64) Economou, I. G.; Tsonopoulos, C. Associating Models and Mixing Rules in Equations of State for Water/Hydrocarbon Mixtures. *Chem. Eng. Sci.* **1997**, *52*, 511−525.
(65) Hudson, G. H.; McCoubrey, J. C. Intermolecular Forces between Unlike Molecules. A More Complete Form of the Combining Rules. *Trans. Faraday Soc.* **1960**, *56*, 761−766.
(66) Rai, N.; Wagner, A. J.; Ross, R. B.; Siepmann, J. I. Application of the TraPPE Force Field for Predicting the Hildebrand Solubility Parameters of Organic Solvents and Monomer Units. *J. Chem. Theory Comput.* **2008**, *4*, 136−144.
(67) Rai, N.; Siepmann, J. I.; Schultz, N. E.; Ross, R. B. Pressure Dependence of the Hildebrand Solubility Parameter and the Internal Pressure: Monte Carlo Simulations for External Pressures up to 300 MPa. *J. Phys. Chem. C* **2007**, *111*, 15634−15641.
(68) Branco, M. C.; Nettesheim, F.; Pochan, D. J.; Schneider, J. P.; Wagner, N. J. Fast Dynamics of Semiflexible Chain Networks of Self-Assembled Peptides. *Biomacromolecules* **2009**, *10*, 1374−1380.
(69) Gao, J.; Tang, C.; Elsawy, M. A.; Smith, A. M.; Miller, A. F.; Saiani, A. Controlling Self-Assembling Peptide Hydrogel Properties through Network Topology. *Biomacromolecules* **2017**, *18*, 826−834.
(70) Pitoňák, M.; Neogrády, P.; Řezáč, J.; Jurečka, P.; Urban, M.; Hobza, P. Benzene Dimer: High-Level Wave Function and Density Functional Theory Calculations. *J. Chem. Theory Comput.* **2008**, *4*, 1829−1834.
(71) Park, Y. C.; Lee, J. S. Accurate Ab Initio Binding Energies of the Benzene Dimer. *J. Phys. Chem. A* **2006**, *110*, 5091−5095.
(72) Headen, T. F.; Howard, C. A.; Skipper, N. T.; Wilkinson, M. A.; Bowron, D. T.; Soper, A. K. Structure of Π−π Interactions in Aromatic Liquids. *J. Am. Chem. Soc.* **2010**, *132*, 5735−5742.
(73) Rai, N.; Siepmann, J. I. Transferable Potentials for Phase Equilibria. 9. Explicit Hydrogen Description of Benzene and Five-Membered and Six-Membered Heterocyclic Aromatic Compounds. *J. Phys. Chem. B* **2007**, *111*, 10790−10799.
(74) Portet, S.; Mücke, N.; Kirmse, R.; Langowski, J.; Beil, M.; Herrmann, H. Vimentin Intermediate Filament Formation: In Vitro Measurement and Mathematical Modeling of the Filament Length Distribution during Assembly. *Langmuir* **2009**, *25*, 8817−8823.
(75) Frisch, M. J.; Trucks, G. W.; Schlegel, H. B.; Scuseria, G. E.; Robb, M. A.; Cheeseman, J. R.; Scalmani, G.; Barone, V.; Mennucci, B.; Petersson, G. A.; et al. *Gaussian 09*; Gaussian, Inc.: Wallingford, CT, 2009.
(76) Zhao, Y.; Truhlar, D. G. The M06 Suite of Density Functionals for Main Group Thermochemistry, Thermochemical Kinetics, Noncovalent Interactions, Excited States, and Transition Elements: Two New Functionals and Systematic Testing of Four M06-Class Functionals and 12 Other Functionals. *Theor. Chem. Acc.* **2007**, *120*, 215−241.
(77) Krishnan, R.; Binkley, J. S.; Seeger, R.; Pople, J. A. Self-consistent Molecular Orbital Methods. XX. A Basis Set for Correlated Wave Functions. *J. Chem. Phys.* **1980**, *72*, 650−654.
(78) McLean, A. D.; Chandler, G. S. Contracted Gaussian Basis Sets for Molecular Calculations. I. Second Row Atoms, Z = 11−18. *J. Chem. Phys.* **1980**, *72*, 5639−5648.
(79) Hariharan, P. C.; Pople, J. A. The Influence of Polarization Functions on Molecular Orbital Hydrogenation Energies. *Theor. Chim. Acta* **1973**, *28*, 213−222.

DOI: 10.1021/acsomega.7b00108
ACS Omega 2017, 2, 1864−1874

(80) Francl, M. M.; Pietro, W. J.; Hehre, W. J.; Binkley, J. S.; Gordon, M. S.; DeFrees, D. J.; Pople, J. A. Self-consistent Molecular Orbital Methods. XXIII. A Polarization-type Basis Set for Second-row Elements. *J. Chem. Phys.* **1982**, *77*, 3654−3665.

DOI: 10.1021/acsomega.7b00108
ACS Omega 2017, 2, 1864−1874